Part V.F: Cosine-Modulated Filter Banks

• This part shows how to efficiently implement a multi-channel ($M > 2$) analysis – synthesis bank using a single prototype filter and a proper cosine modulation scheme.

• It is mostly based on the following article: T. Saramäki, "A generalized class of cosine-modulated filter banks," in *Transforms and Filter Banks. Proceedings of First International Workshop on Transforms and Filter Banks* (Tampere, Finland), edited by K. Egiazarian, T. Saramäki, and J. Astola, pp. 336-365, 1998.

Organization of This Pile of Lecture Notes

• This pile can be roughly divided into the the following subparts:

1. Introduction

2. Cosine-modulated FIR filter banks

3. Nearly perfect-reconstruction filter banks

4. Perfect-reconstruction filter banks

5. Filter banks with constraints on the amplitude distortion

6. Filter banks with constraints on both the amplitude and aliasing distortions

7. Practical examples

8. Implementation aspects

1. Introduction

• During the past ten years, the subband coding by M-channel critically sampled FIR filter banks have received a widespread attention [1], [2], [3] (see also references in these textbooks).

• Such a system is shown in Fig. 1.

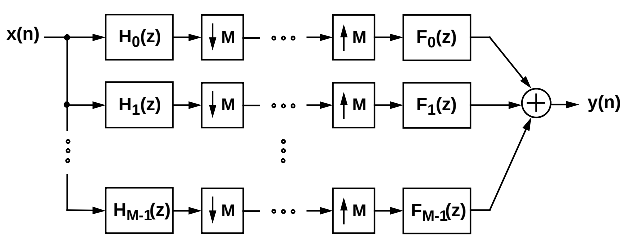

Figure 1: M-channel maximally decimated filter bank.

• In the analysis bank consisting of M parallel bandpass filters $H_k(z)$ for $k = 0, 1, \cdots, M-1$ ($H_0(z)$ and $H_{M-1}(z)$ are lowpass and highpass filters, respectively), the input signal is filtered by these filters into separate subband signals.

• These signals are individually decimated by M, quantized, and edcoded for transmission to the synthesis bank consisting also of M parallel filters $F_k(z)$ for $k = 0, 1, \cdots, M-1$.

• In the synthesis bank, the coded symbols are converted to their appropriate digital quantities, interpolated by a factor of M followed by filtering by the corresponding filters $F_k(z)$.

• Finally, the outputs are added to produce the quantized version of the input.

• These filter banks are used in a number of communication applications such as subband coders for speech signals, frequency-domain speech scramblers, image coding, and adaptive signal processing [1].

• The most effective technique for constructing both the analysis bank consisting of filters $H_k(z)$ for $k = 0, 1, \cdots, M-1$ and the synthesis bank consisting of filters $F_k(z)$ for $k = 0, 1, \cdots, M-1$ is to use a cosine modulation [1], [2], [3] to generated both banks from a single linear-phase FIR prototype filter.

• Compared to the case where all the subfilters are designed and implemented separately, the implementation of both the analysis and synthesis banks is significantly more efficient since it requires only one prototype filter and a unit performing the desired modulation operation [1], [2], [3].

• Also, the actual filter bank design becomes much faster and more straightforward since the only parameters to be optimized are the coefficients of a single prototype filter.

• Another alternative is to use the modified DFT [3].

• However, this is a very new idea lacking a good tutorial article. Therefore, this alternative is not considered in this course.

• The purpose of this pile of lecture notes is to introduce efficient design techniques for generating prototype filters for both perfect-reconstruction and nearly perfect-reconstruction cases using a cosine modulation.

• Several examples are included illustrating that by allowing small amplitude and aliasing errors, the filter bank performance can be significantly improved.

• Alternatively, the filter orders and the overall delay caused by the filter bank to the signal can be considerably reduced. This is very important in communication applications.

• In many applications such small errors are tolerable and the distortion caused by these errors to the signal is smaller than that caused by coding.

2. Cosine-Modulated FIR Filter Banks

• This section shows how M-channel critically sampled FIR filter banks can be generated using proper cosine-modulation techniques and a proper prototype filter.

2.1 Input-Output Relation for an M-Cannel Filter Bank

• For the system of Fig. 1, the input-output relation in the z-domain is expressible as

$$Y(z) = T_0(z)X(z) + \sum_{l=1}^{M-1} T_l(z)X(ze^{-j2\pi l/M}), \qquad (1a)$$

where

$$T_0(z) = \frac{1}{M}\sum_{k=0}^{M-1} F_k(z)H_k(z) \qquad (1b)$$

and for $l = 1, 2, \cdots, M-1$

$$T_l(z) = \frac{1}{M}\sum_{k=0}^{M-1} F_k(z)H_k(ze^{-j2\pi l/M}). \qquad (1c)$$

• Here, $T_0(z)$ is called the distortion transfer function and determines the distortion caused by the overall system for the unaliased component $X(z)$ of the input signal.

• The remaining transfer functions $T_l(z)$ for $l = 1, 2, \cdots, M-1$ are called the alias transfer functions and determine how well the aliased components $X(ze^{-j2\pi l/M})$ of the input signal are attenuated.

• For the perfect reconstruction, it is reguired that $T_0(z) = z^{-N}$ with N being an integer and $T_l(z) = 0$ for $l = 1, 2, \cdots, M-1$.

• If these conditions are satisfied, then the output signal is a delayed version of the input signal, that is, $y(n) = x(n-N)$.

• It should be noted that the perfect reconstruction is exactly achieved only in the case of lossless coding.

• For lossy coding, it is worth studing whether it is beneficial to allow small amplitude and aliasing errors causing smaller distortions to the signal than the coding or errors that are not very noticable in practical applications.

• For nearly perfect reconstruction cases, the abovementioned conditions should be satisfied within given tolerances.

• The term $1/M$ in Eqs. (1b) and (1c) is a consequence of the decimation and interpolation processes.

• For simplicity, this term is forgotten in the sequel.

• In this case, the passband maxima of the amplitude responses of the $H_k(z)$'s and $F_k(z)$'s will become approximately equal to unity.

• Also the prototype filter to be considered later on can be designed such that its amplitude response has

approximately the value of unity at the zero frequency.

• The desired input-output relation is then achieved in the final implementation by multiplying the $F_k(z)$'s by M.

• This is done in order to preserve the signal energy after using the interpolation filters $F_k(z)$.

• In this case, the filters in the analysis and synthesis banks of the overall system become approximately peak scaled, as is desired in many practical applications.

2.2 Generation of Filter Banks from a Prototype Filter Using Cosine-Modulation Techniques

• For the cosine-modulated filter banks, both the $H_k(z)$'s and $F_k(z)$'s are constructed with the aid of a linear-phase FIR prototype filter of the form

$$H_p(z) = \sum_{n=0}^{N} h_p(n) z^{-n}, \tag{2a}$$

where the impulse response satisfies the following symmetry property:

$$h_p(N-n) = h_p(n). \tag{2b}$$

• One alternative is to construct them as follows [2]:

$$H_k(z) = \alpha_k \beta_k H_p(ze^{-j(2k+1)\pi/(2M)}) + \alpha_k^* \beta_k^* H_p(ze^{j(2k+1)\pi/(2M)}) \tag{3a}$$

and

$$F_k(z) = \alpha_k^* \beta_k H_p(ze^{-j(2k+1)\pi/(2M)}) + \alpha_k \beta_k^* H_p(ze^{j(2k+1)\pi/(2M)}, \tag{3b}$$

where $\alpha_k = e^{j(-1)^k \pi/4}$ and $\beta_k = e^{-jN(2k+1)\pi/(4M)}$.

• The corresponding impulse responses for $k = 0, 1, \cdots, M-1$ are then given by

$$h_k(n) = 2h_p(n) \cos[(2k+1)\frac{\pi}{2M}(n - \frac{N}{2}) + (-1)^k \frac{\pi}{4}] \tag{4a}$$

and

$$f_k(n) = 2h_p(n) \cos[(2k+1)\pi 2M(n - \frac{N}{2}) - (-1)^k \frac{\pi}{4}]. \tag{4b}$$

• From the above equations, it follows that for $k = 0, 1, \cdots, M-1$

$$f_k(n) = h_k(N-n) \tag{5a}$$

and

$$F_k(z) = z^{-N} H_k(z^{-1}). \tag{5b}$$

• Another alternative is to construct the impulse responses $h_k(n)$ and $f_k(n)$ as follows [1]:

$$f_k(n) = 2h_p(n) \cos[\frac{\pi}{2M}(k + \frac{1}{2})(n + \frac{M+1}{2})] \tag{6a}$$

and

$$h_k(n) = f_k(N-n) = 2h_p(n) \cos[\frac{\pi}{2M}(k+\frac{1}{2})(N-n+\frac{M+1}{2})]. \tag{6b}$$

• In [1], instead of the constant of value 2, the constant of value $\sqrt{2/M}$ has been used. The reason for this is that the prototype filter is implemented using special butterflies.

• The most important property of the above modulation schemes lies in the following facts.

• By properly designing the prototype filter transfer function $H_p(z)$, the aliased components generated in the analysis bank due to the decimation can be totally or partially compensated in the synthesis bank.

• Secondly, $T_0(z)$ can be made exactly or approximately equal to the pure delay z^{-N}.

• Hence, these modulation techniques enable us to design the prototype filter in such a way that the resulting overall bank has the perfect-reconstruction or a nearly perfect-reconstruction property.

2.3 Conditions for the Prototype Filter to Give a Nearly Perfect-Reconstruction Property

• The above modulation schemes guarantee that if the impulse response of

$$\widehat{H}_p(z) = [H_p(z)]^2 = \sum_{n=0}^{2N} \widehat{h}_p(n) z^{-n}, \quad \widehat{h}_p(2N-n) = \widehat{h}_p(n) \tag{7a}$$

satisfies ($\lfloor x \rfloor$ stands for the integer part of x.)

$$\widehat{h}_p(N) \approx 1/(2M) \tag{7b}$$

and

$$\widehat{h}_p(N \pm 2rM) \approx 0 \quad \text{for} \quad r = 1, 2, \cdots, \lfloor N/(2M) \rfloor, \tag{7c}$$

then [4]

$$T_0(z) = \sum_{l=0}^{M-1} F_k(z) H_k(z) \approx z^{-N}. \tag{8}$$

• In this case, the amplitude error $|T_0(e^{j\omega}) - e^{-jN\omega}|$ becomes very small.

• If the conditions of Eqs. (7b) and (7c) are exactly satisfied, then the the amplitude error becomes zero.

• It should be noted that since $T_0(z)$ is an FIR filter of order $2N$ and its impulse-response coefficients, denoted by $t_0(n)$, satisfy $t_0(2N-n) = t_0(n)$ for $n = 0, 1, \cdots, 2N$, there exists no phase distortion.

• Equation (7) implies that $[H_p(z)]^2$ is approximately a $2M$th-band linear-phase FIR filter [5], [6].

• Based on the properties of these filters, the stopband edge of the prototype filter $H_p(z)$ must be larger than $\pi/(2M)$ and is specified by

$$\omega_s = (1+\rho)\pi/(2M), \tag{9}$$

where $\rho > 0$.

• Furthermore, the amplitude response of $H_p(z)$ achieves approximately the values of unity and $1/\sqrt{2}$ at $\omega = 0$ and $\omega = \pi/(2M)$, respectively.

• As an example, Fig. 2 shows the prototype filter frequency response for $M = 4$, $N = 63$, and $\rho = 1$ as well as the responses for the filters $H_k(z)$ and $F_k(z)$ for $k = 0, 1, 2, 4$.

• It is seen that the filters $H_k(z)$ and $F_k(z)$ for $k = 1, 2, \cdots, M-2$ are bandpass filters with the center frequency at $\omega = \omega_k = (2k+1)\pi/(2M)$ around which the amplitude response is very flat having approximately the value of unity.

• The amplitude response of these filters achieves approximately the value of $1/\sqrt{2}$ at $\omega = \omega_k \pm \pi/(2M)$ and the stopband edges are at $\omega = \omega_k \pm \omega_s$.

• $H_0(z)$ and $F_0(z)$ [$H_{M-1}(z)$ and $F_{M-1}(z)$] are lowpass (highpass) filters with the amplitude response being flat around $\omega = 0$ ($\omega = \pi$) and achieving approximately the value $1/\sqrt{2}$ at $\omega = \pi/M$ ($\omega = \pi - \pi/M$).

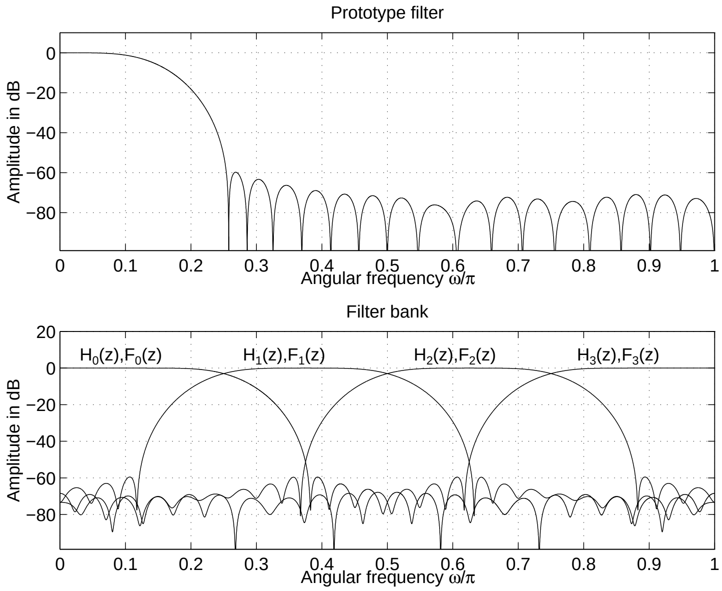

Figure 2: Example amplitude responses for the prototype filter and for the resulting filters in the analysis and synthesis banks for $M = 4$, $N = 63$, and $\rho = 1$.

• The stopband edge is at $\omega = (2+\rho)\pi/(2M)$ [$\omega = \pi - (2+\rho)\pi/(2M)$].

• The impulse responses for the prototype filter as well as those for the filters in the banks are shown in Figs. 3 and 4, respectively.

• In this case, the impulse responses for the filtes in the bank have been generated according to Eq. (4).

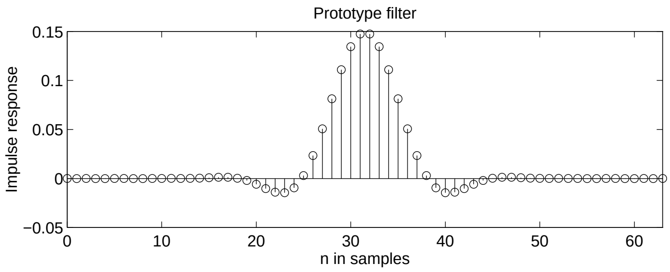

Figure 3: Impulse response for the prototype filter in the case of Fig. 2.

• If $H_p(z)$ satisfies Eq. (7), then both of the abovementioned modulation schemes have the very important property that the maximum amplitude values of the aliased transfer functions $T_l(z)$ for $l = 1, 2, \cdots, M-1$ are guaranteed to be approximately equal to the maximum stopband amplitude values of the filters in the bank [2], as will be seen in connection with the examples of Section 5.

• If smaller aliasing error levels are desired to be achieved, then additional constraints must be imposed on the prototype filter.

• This will be considered in the next section.

• In the case of the perfect reconstruction, the additional constraints are so strict that they actually reduce the number of adjustable parameters of the prototype filter, as will be seen in Section 4.

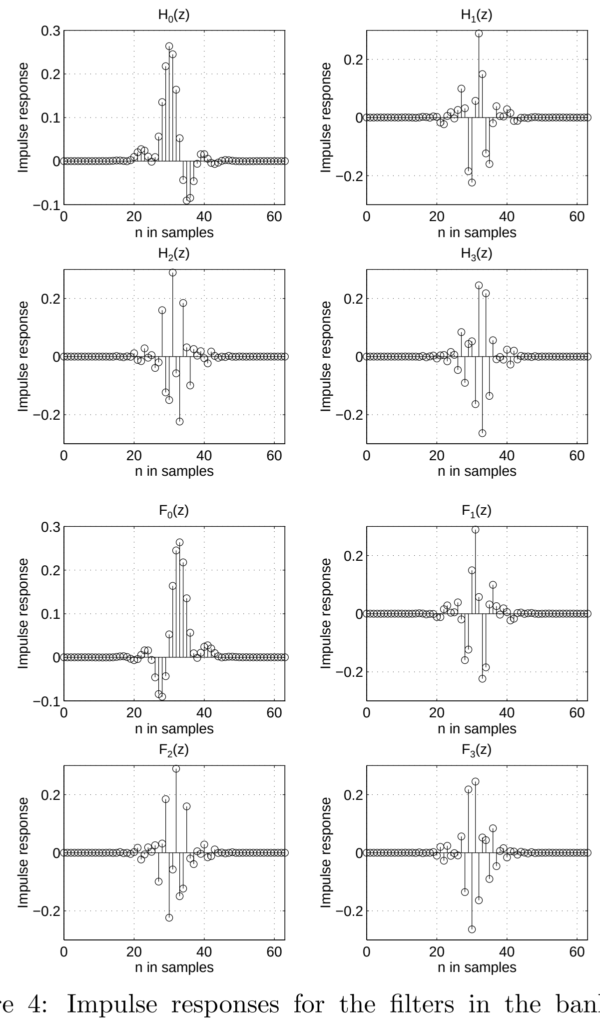

Figure 4: Impulse responses for the filters in the bank in the case of Fig. 2.

3 General Optimization Problems for the Prototype Filter

- This section states two optimization problems for designing the prototype filter in such a way that the overall filter bank possesses a nearly perfect-reconstruction property.
- Efficient algorithms are then briefly described for solving these problems.

3.1 Statement of the Problems

- We consider the following two general optimization problems:

Problem I. Given ρ, M, and N, find the coefficients of $H_p(z)$ to minimize

$$E_2 = \int_{\omega_s}^{\pi} |H_p(e^{j\omega})|^2 d\omega, \qquad (10a)$$

where

$$\omega_s = (1+\rho)\pi/(2M) \qquad (10b)$$

subject to

$$1 - \delta_1 \le |T_0(e^{j\omega})| \le 1 + \delta_1, \quad \omega \in [0,\ \pi] \qquad (10c)$$

and

$$|T_l(e^{j\omega})| \le \delta_2, \quad \omega \in [0,\ \pi] \quad \text{for} \quad l = 1, 2, \cdots, M-1. \qquad (10d)$$

Problem II. Given ρ, M, and N, find the coefficients of $H_p(z)$ to minimize

$$E_\infty = \max_{\omega \in [\omega_s,\ \pi]} |H_p(e^{j\omega})| \qquad (11)$$

subject to the conditions of Eqs. (10c) and (10d).

3.2 Algorithm for Solving Problem I

- This contribution concentrates on the case where N, the order of the prototype filter, is odd (the length $N+1$ is even).
- This is because for the perfect-reconstruction case N is restricted to be odd, as will be seen in the following section.
- For N odd, the frequency response of the prototype filter is expressible as

$$H_p(\Phi, e^{j\omega}) = 2e^{-j(N-1)\omega/2} \sum_{n=1}^{(N+1)/2} h_p[(N+1)/2 - n] \cos[(n-1/2)\omega], \qquad (12a)$$

where

$$\Phi = [h_p(0), h_p(1), \cdots, h[(N-1)/2] \qquad (12b)$$

denotes the adjustable parameter vector of the prototype filter.

- After some manipulations, Eq. (10a) is expressible as

$$E_2(\Phi) \equiv E_2 = \sum_{\mu=1}^{(N+1)/2} \sum_{\nu=1}^{(N+1)/2} h_p[(N+1)/2 - \mu] h_p[(N+1)/2 - \nu] \Psi(\mu, \nu), \qquad (13a)$$

where

$$\Psi(\mu,\nu) = 4\int_{\omega_s}^{\pi} \cos(\mu - 1/2)\cos(\nu - 1/2) d\omega$$

$$= \begin{cases} 2\pi - 2\omega_s - \dfrac{2\sin[(2\mu-1)\omega_s]}{2\mu - 1}, & \mu = \nu \\ -\dfrac{2\sin[(\mu+\nu-1)\omega_s]}{\mu+\nu-1} - \dfrac{2\sin[(\mu-\nu)\omega_s]}{\mu-\nu}, & \mu \ne \nu \end{cases}. \qquad (13b)$$

- $|T_l(\Phi, e^{j\omega})|$ for $l = 0, 1, \cdots, M-1$, in turn, can be written as shown in the article mentioned in the first page of this part of lecture notes.
- To solve Problem I, we discretize the region $[0, \pi/M]$ into the discrete points $\omega_j \in [0, \pi/M]$ for $j = 1, 2, \cdots, J_0$.
- In many cases, $J_0 = N$ is a good selection to arrive at a very accurate solution.
- The resulting discrete problem is to find Φ to minimize

$$\epsilon = E_2(\Phi), \qquad (14a)$$

where $E_2(\Phi)$ is given by Eq. (13) subject to

$$g_j(\Phi) \le 0, \quad j = 1, 2, \cdots, J, \qquad (14b)$$

where

$$J = \lfloor (M+2)/2 \rfloor J_0, \qquad (14c)$$

$$g_j(\Phi) = ||T_0(\Phi, e^{j\omega_j})| - 1| - \delta_1, \quad j = 1, 2, \cdots, J_0, \qquad (14d)$$

and

$$g_{lJ_0+j}(\Phi) = |T_l(\Phi, e^{j\omega_j})| - \delta_2, \quad l = 1, 2, \cdots, \lfloor M/2 \rfloor, \quad j = 1, 2, \cdots, J_0. \tag{14f}$$

- In the above, the region $[0, \pi/M]$, instead of $[0, \pi]$, has been used since the $|T_l(\Phi, e^{j\omega})|$'s are periodic with periodicity equal to $2\pi/M$.
- Furthermore, only the first $\lfloor (M+2)/2 \rfloor$ $|T_l(\Phi, e^{j\omega})|$'s have been used since $|T_l(\Phi, e^{j\omega})| = |T_{M-l}(\Phi, e^{j\omega})|$ for $l = 1, 2, \cdots, \lfloor (M-1)/2 \rfloor$.
- The above problem can be solved conveniently by using the second algorithm of Dutta and Vidyasagar [7]. The details can be found in the article mentioned in the first page of this part of lecture notes.
- Since the optimization problem is nonlinear in nature, a good initial starting point for the vector Φ is needed.
- This can be obtained by finding a corresponding vector in the perfect-reconstruction case to be considered in the next section.
- If it is desired that $|T_0(\Phi, e^{j\omega})| \equiv 1$ [4], then the resulting discrete problem is to find Φ to minimize ϵ as given by Eq. (14a) subject to

$$g_j(\Phi) \le 0, \quad j = 1, 2, \cdots, J \tag{15a}$$

and

$$h_l(\Phi) = 0, \quad l = 1, 2, \cdots, L, \tag{15b}$$

where

$$J = \lfloor M/2 \rfloor J_0, \tag{15c}$$

$$L = J_0,$$

$$g_{(l-1)J_0+j}(\Phi) = |T_l(\Phi, e^{j\omega_j})| - \delta_2, \quad l = 1, 2, \cdots, \lfloor M/2 \rfloor, \quad j = 1, 2, \cdots, J_0, \tag{15d}$$

and

$$h_l(\Phi) = ||T_0(\Phi, e^{j\omega_j})| - 1|, \quad l = 1, 2, \cdots, L. \tag{15e}$$

- This problem can also be solved conveniently using the Dutta-Vidyasagar algorithm.

3.3 Algorithm for Solving Problem II

- To solve Problem II, we discretize the region $[\omega_s, \pi]$ into the discrete points $\omega_i \in [\omega_s, \pi]$ for $i = 1, 2, \cdots, I$.
- In many cases, $I = 20N$ is a good selection. The resulting discrete minimax problem is to find Φ to minimize

$$\epsilon = \widehat{E}_\infty(\Phi) = \max_{i \in I} f_i(\Phi) \tag{16a}$$

subject to

$$g_j(\Phi) \le 0, \quad j = 1, 2, \cdots, J, \tag{16b}$$

where

$$f_i(\Phi) = |H_p(\Phi, e^{j\omega_i})|, \quad i = 1, 2, \cdots, I \tag{16c}$$

and J and the $g_j(\Phi)$'s are given by Eqs. (14c), (14d), and (14e).

- Again, the Dutta-Vidyasagar algorithm can be used to solve the above problem.
- Also, the optimization of the prototype filter for the case where $|T_0(\Phi, e^{j\omega})| \equiv 1$ can be solved like for Problem I.
- Similarly, a good initial vector Φ is obtained by finding a corresponding vector for the perfect-reconstruction case.

4. Perfect-Reconstruction Filter Banks

- This section introduces algorithms for designing effectively the prototype filter for perfect-reconstruction filter banks either in the least-mean-square sense or in the minimax sense.
- Both of these algorithms are characterized by the desired property that they enable us to design banks of filters with much higher lengths than the other existing synthesis techniques.

4.1 Conditions for the Perfect Reconstruction

- Under certain conditions, the output of the filter bank is a delayed version of the output. These conditions are $T_0(z) \equiv z^{-N}$ and $T_l(z) \equiv 0$ for $l = 1, 2, \cdots, M-1$ [8]–[14].
- In this case, $N + 1 = 2KM$ with K being an integer and only $K\lfloor M/2 \rfloor$ parameters are adjustable.
- In the sequel, the conditions for the prototype filter are given in the form suggested in [13]. This form can be used in a straightforward manner in optimizing the prototype filter in the minimax or in the least mean-square sense.
- The suggested form for the perfect reconstruction has been derived by slightly modifying the conditions given in [10].

• In the following subsection, the connections of this form to those described in [10], [11] will be given.

• The prototype filter transfer function as given by Eq. (2) can be expressed as

$$H_p(z) = G_p(z)/(M\sqrt{2}), \qquad (17a)$$

where

$$G_p(z) = z^{-(KM-1/2)} \sum_{n=1}^{KM} g(n)[z^{(n-1/2)} + z^{-(n-1/2)}]. \qquad (17b)$$

• Here, the $h_p(n)$'s are related to the $g(n)$'s through

$$h_p(n) = h_p(2KM-1-n) = g(KM-n)/(M\sqrt{2}) \quad \text{for} \quad n = 0,1,\cdots,KM-1. \qquad (18)$$

• The basic reason for expressing the prototype filter transfer function in the above form lies in the fact that the conditions for the perfect reconstruction can be stated conveniently with the aid of the $g(n)$'s for $n = 1,2,\cdots,KM$.

• First, these conditions imply that for M odd,

$$g((M+1)/2) = \sqrt{1/2} \qquad (19a)$$

and

$$g((M+1)/2 + kM) = 0 \text{ for } k = 1,2,\cdots,K-1. \qquad (19b)$$

• For M even, this condition is absent.

• Second, there are K constraints for each of the remaining $\lfloor M/2 \rfloor$ sets of $2K$ $g(n)$'s.

• These sets are given by

$$\Theta_r = \{g(r), g(M+1-r), g(M+r), g(2M+1-r), g(2M+r), g(3M+1-r), \cdots, g((K-1)M+r), g(KM+1-r)\} \quad \text{for} \quad r = 1,2,\cdots,\lfloor M/2 \rfloor. \qquad (20)$$

• For the rth set Θ_r, the conditions can be expressed in a convenient manner in terms of

$$c_{rk} = \cos(\phi_{rk}) \qquad (21a)$$

and

$$s_{rk} = \sin(\phi_{rk}), \qquad (21b)$$

where the ϕ_{rk}'s for $k = 1,2,\ldots,K$ are the basic adjustable parameters.

• To do this, the following $(K-1)$th-order polynomials in z^{-1} are first determined:

$$P_r^{(K)}(z) = \sum_{n=0}^{K-1} p_r(n) z^{-n} \qquad (22a)$$

and

$$Q_r^{(K)}(z) = \sum_{n=0}^{K-1} q_r(n) z^{-n} \qquad (22b)$$

recursively as

$$P_r^{(k)}(z) = s_{rk} P_r^{(k-1)}(z) + c_{rk} z^{-1} Q_r^{(k-1)}(z) \qquad (23a)$$

and

$$Q_r^{(k)}(z) = c_{rk} P_r^{(k-1)}(z) - s_{rk} z^{-1} Q_r^{(k-1)}(z) \qquad (23b)$$

with the initializations

$$P_r^{(1)}(z) = s_{r1} \qquad (23c)$$

and

$$Q_r^{(1)}(z) = c_{r1}. \qquad (23d)$$

• For K even, the desired conditions take then the following form:

$$g(2kM+r) = p_r(\frac{K}{2}+k) \quad \text{for} \quad k = 0,1,\cdots,\frac{K}{2}-1, \qquad (24a)$$

$$g((2k+1)M+r) = q_r(\frac{K}{2}+k) \quad \text{for} \quad k = 0,1,\cdots,\frac{K}{2}-1, \qquad (24b)$$

$$g(2kM+1-r) = p_r(\frac{K}{2}-k) \quad \text{for} \quad k = 1,2,\cdots,\frac{K}{2}, \qquad (24c)$$

and

$$g((2k-1)M+1-r) = q_r(\frac{K}{2}-k) \quad \text{for} \quad k = 1,2,\cdots,\frac{K}{2}. \qquad (24d)$$

• For K odd, they become

$$g(2kM+r) = q_r(\frac{K-1}{2}+k) \quad \text{for} \quad k = 0,1,\cdots,\frac{K-1}{2}, \qquad (25a)$$

$$g((2k-1)M+r) = p_r(\frac{K-1}{2}+k) \quad \text{for} \quad k = 1,2,\cdots,\frac{K-1}{2}, \qquad (25b)$$

$$g(2kM+1-r) = q_r(\frac{K-1}{2}-k) \quad \text{for} \quad k = 1,2,\cdots,\frac{K-1}{2}, \qquad (25c)$$

and

$$g((2k+1)K+1-r) = p_r(\frac{K-1}{2}-k) \quad \text{for} \quad k = 0,1,\cdots,\frac{K-1}{2}. \qquad (25d)$$

• The key point for using the ϕ_{rk}'s as the basic adjustable parameters lies in the fact that for any selection of these parameters the perfect-recontruction property can be achieved.

• The zero-phase frequency response of the filter with the transfer function $G_p(z)$ can be written in terms of the $g(n)$'s as

$$G_p(\Phi,\omega) = 2\sum_{n=1}^{KM} g(n,\Phi)\cos[(n-1/2)\omega], \qquad (26a)$$

where Φ is an $K\lfloor M/2 \rfloor$ length vector containing the adjustable parameters ϕ_{rk} for $r = 1,2,\cdots,\lfloor M/2 \rfloor$ and $k = 1,2,\cdots,K$, that is,

$$\Phi = [\phi_{11}, \phi_{12}, \cdots, \phi_{1K}, \phi_{21}, \phi_{22}, \cdots, \phi_{2K}, \cdots, \phi_{\lfloor M/2 \rfloor,1}, \phi_{\lfloor M/2 \rfloor,2}, \cdots, \phi_{\lfloor M/2 \rfloor,K}]. \qquad (26b)$$

• The above notations are used to emphasize the dependences of $g(n,\Phi)$ and $G_p(\Phi,\omega)$ on the basic adjustable parameters.

4.2 Relations of the Proposed Adjustable Angles to Those of Existing Implementation Forms

• There are very simple relations of the angles ϕ_{rk} to the corresponding angles used by Malvar in [14] and Koilpillai and Vaidyanthan in [10] for generating perfect-recontruction cosine-modulated filter banks.

• For the angles considered in [14], denoted by θ_{rk} for $r = 0, 1\cdots, \lfloor M/2 \rfloor - 1$ and $k = 0, 1, \cdots, K-1$, the relations are given by

$$\theta_{r,2k} = 3\pi/2 - \phi_{r+1,K-2k} \text{ for } k = 0, 1, \cdots, \lfloor K/2 - 1 \rfloor \quad (27a)$$

and

$$\theta_{r,2k+1} = \pi/2 + \phi_{r+1,K-2k-1} \text{ for } k = 0, 1, \cdots, \lfloor K/2 \rfloor - 1 \quad (27b)$$

for K even.

• For K odd, the corresponding relations take the following form:

$$\theta_{r,2k} = \pi/2 + \phi_{r+1,K-2k} \text{ for } k = 0, 1, \cdots, \lfloor K/2 \rfloor \quad (28a)$$

and

$$\theta_{r,2k+1} = 3\pi/2 - \phi_{r+1,K-2k-1} \text{ for } k = 0, 1, \cdots, \lfloor K/2 \rfloor - 1. \quad (28b)$$

• For the corresponding angles considered in [10], again denoted by θ_{rk} for $r = 0, 1\cdots, \lfloor M/2 \rfloor - 1$ and $k =$

$0, 1, \cdots, K-1$, the desired relations have the following simple form:

$$\theta_{r,k} = \pi/2 - \phi_{r+1,k+1}. \quad (29)$$

4.3 Optimization Problems

• We consider the following two optimization problems:

Problem A. Given M, K, and ρ, find the unknowns ϕ_{rk} for $r = 1, 2, \cdots, \lfloor M/2 \rfloor$ and $k = 1, 2, \cdots, K$ to minimize

$$E_2(\Phi) = \int_{\omega_s}^{\pi} [G_p(\Phi, \omega)]^2 d\omega, \quad (30a)$$

where

$$\omega_s = (1+\rho)\pi/(2M). \quad (30b)$$

Problem B. Given M, K, and ρ, find the unknowns ϕ_{rk} for $r = 1, 2, \cdots, \lfloor M/2 \rfloor$ and $k = 1, 2, \cdots, K$ to minimize

$$E_\infty = \max_{\omega \in [\omega_s,\ \pi]} |G_p(\Phi, \omega)| \quad (31)$$

• In the first case, the stopband energy of the prototype filter is minimized, whereas in the second case the maximum deviation of the amplitude response from zero in the stopband region is minimized.

4.4 Design Algorithm for Problem A

• For Problem A, the objective function can be expressed, after some manipulations, in the form

$$E_2(\Phi) = \sum_{\mu=1}^{KM} \sum_{\nu=1}^{KM} g(\mu, \Phi) g(\nu, \Phi) \Psi(\mu, \nu), \quad (32)$$

where $\Psi(\mu, \nu)$ is given by Eq. (13b).

• The partial derivatives of $E_2(\Phi)$ with respect to the unknowns ϕ_{rn} $r = 1, 2, \cdots, \lfloor M/2 \rfloor$ and $n = 1, 2, \cdots, K$ are given by

$$\frac{\partial E_2(\Phi)}{\partial \phi_{rn}} = 2 \sum_{\mu=1}^{KM} \sum_{\nu=1}^{KM} \widehat{g}_{rn}(\mu, \Phi) g(\nu, \Phi) \Psi(\mu, \nu), \quad (33a)$$

where

$$\widehat{g}_{rn}(\mu, \Phi) = \frac{\partial g(\mu, \Phi)}{\partial \phi_{rn}}. \quad (33b)$$

• Only the elements $\widehat{g}_{nk}((k-1)M + r, \Phi)$ and $\widehat{g}(kM + r, \Phi)$ for $k = 1, 2, \cdots, K$ are nonzero.

• The values of these elements can be determined with the aid of the angles ϕ_{rk} for $k = 1, 2, \cdots, K$ like those of the elements $g((k-1)M + r, \Phi)$ and $g(kM + r, \Phi)$ for $k = 1, 2, \cdots, K$ according to Eqs. (21)–(25).

• The only exeption is that for $k = n$ $c_{rn} = -\sin(\phi_{rn})$ and $s_{rk} = \cos(\phi_{rn})$.

• Knowing the partial derivates with respect to the unknows, the optimum solution can be found in a straightforward manner using, for instance, the Fletcher-Powell algorithm [15].

• The main advantage of the above formulation of the optimization problem is the fact that when changing the unknown angles during optimization, the overall filter bank is guaranteed to have all the time the perfect-recontruction property without having additional constraints.

4.5 Practical Filter Design for Problem A

• This subsection illustrates, by means of an example, how to design effectively a cosine-modulated filter bank for large values of K and M.

• It is desired to design a bank with $M = 32$ filters of length $N+1 = 512$ $(K = 8)$ for $\rho = 1$.

• A very fast procedure to arrive at least at a local optimum is the following (see Fig. 5):

Step 1: Optimize the prototype filter for $M = 2$, $K = 8$, and $\rho = 1$ using the initial values $\phi_{1k}^{(0)} = 0$ for $k = 1, 2, \cdots, 8$.

Step 2: Optimize the filter for $M = 4$, $K = 8$, and $\rho = 1$ using the initial values $\phi_{rk}^{(2)} = \phi_{1k}^{(1)}$ for $r = 1, 2$ and $k = 1, 2, \cdots, 8$, where the $\phi_{1k}^{(1)}$'s are the optimized parameters of the previous step.

Step 3: Optimize the filter for $M = 8$, $K = 8$, and $\rho = 1$ using the initial values $\phi_{rk}^{(3)} = \phi_{1k}^{(2)}$ for $r = 1, 2$ and $\phi_{rk}^{(3)} = \phi_{2k}^{(2)}$ for $r = 3, 4$, where the $\phi_{1k}^{(2)}$'s are the optimized parameters of the previous step.

Step 4: Optimize the filter for $M = 16$, $K = 8$, and $\rho = 1$ using the initial values $\phi_{rk}^{(4)} = \phi_{1k}^{(3)}$ for $r = 1, 2$, $\phi_{rk}^{(4)} = \phi_{2k}^{(3)}$ for $r = 3, 4$, $\phi_{rk}^{(4)} = \phi_{3k}^{(3)}$ for $r = 5, 6$, and $\phi_{rk}^{(4)} = \phi_{4k}^{(3)}$ for $r = 7, 8$, where the $\phi_{1k}^{(3)}$'s are the optimized parameters of the previous step.

Step 5: Optimize the filter for $M = 32$, $K = 8$, and $\rho = 1$ using the initial values $\phi_{rk}^{(5)} = \phi_{1k}^{(4)}$ for $r = 1, 2$, $\phi_{rk}^{(5)} = \phi_{2k}^{(4)}$ for $r = 3, 4$, $\phi_{rk}^{(5)} = \phi_{3k}^{(4)}$ for $r = 5, 6$, $\phi_{rk}^{(5)} = \phi_{4k}^{(4)}$ for $r = 7, 8$, $\phi_{rk}^{(5)} = \phi_{5k}^{(4)}$ for $r = 9, 10$, $\phi_{rk}^{(5)} = \phi_{6k}^{(4)}$ for $r = 11, 12$, $\phi_{rk}^{(5)} = \phi_{7k}^{(4)}$ for $r = 13, 14$, and $\phi_{rk}^{(5)} = \phi_{8k}^{(4)}$ for $r = 15, 16$. Here, where the $\phi_{1k}^{(4)}$'s are the optimized parameters of the previous step.

• For the initial filter at Step 1, $g(1) = 1$ and $g(n) = 0$ for $n = 2, 3, \cdots, KM = 8$.

• Correspondingly, $h_p(KM-1) = h_p(KM) = 1/(2\sqrt{2})$ and the remaining impulse response values are zero.

• This has turned out to be a good starting point filter at Step 1.

• The basic idea of performing Steps 2, 3, 4, and 5 as described above lies in the fact that the transfer function obtained using the given initial values is expressible as

$$H_p(z) = \widetilde{H}_p(z^2)(1 + z^{-1})/2, \tag{34}$$

where $\widetilde{H}_p(z)$ is the transfer function optimized at the previous step.

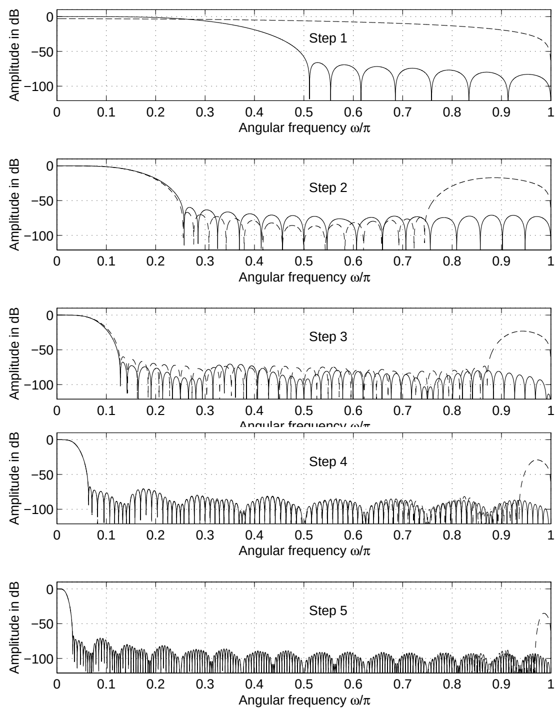

Figure 5: Design a perfect-reconstruction prototype filter using a five-step procedure for $M = 32$, $N+1 = 512$, and $\rho = 1$. The dashed and solid lines show the initial and optimized responses, respectively.

• As seen from Fig. 5, this means that the amplitude response of $\widetilde{H}_p(z^2)$ is a frequency-axis compressed version of that of $\widetilde{H}(z)$ in such a way that the interval

$[0, 2\pi]$ is shrunk onto $[0, \pi]$.

- Therefore, it has an extra passband at $\omega = \pi$. This is partially attenuated by the term $(1 + z^{-1})/2$.
- After the optimization, the extra peak around $\omega = \pi$ is attenuated.
- It is interesting to observe from Fig. 5 that as M is increased, the term $(1 + z^{-1})/2$ provides a better attenuation and the initial filter becomes close to the optimized one.
- The above procedure enables us to design very fast at least suboptimum filters for very high values of K and M compared to the case where the overall filter is designed using only a one-step procedure.
- In the time domain, Eq. (34) means that the impulse response of $H_p(z)$ is related to that of $\widetilde{H}_p(z)$ through

$$\widetilde{h}_p(2n) = \widetilde{h}_p(2n+1) = h_p(n)/2 \quad \text{for} \quad n = 0, 1, \cdots, \widetilde{N}_p, \tag{35}$$

where $\widetilde{N}_p$ is the order of $\widetilde{H}_p(z)$.

- As seen from Fig. 6, the impulse response of the initial filter is obtained from the optimized impulse response of the previous step in two steps.
- First, the impulse-response values are divided by two.
- Then, the resulting values are repeated two times, increasing the length of the resulting filter by a factor of

two.

- After the optimization, this impulse response becomes smooth as seen from Fig. 6.
- Figure 7 shows in the perfect-reconstruction case the prototype filter designed in the least-mean-square sense as well as the filters in the bank for $M = 32$, $N = 512$, and $\rho = 1$.
- Some characteristics of the resulting filter bank can be found in Table I.
- In this table, the characteristics of the filter banks to be considered later on will be collected.

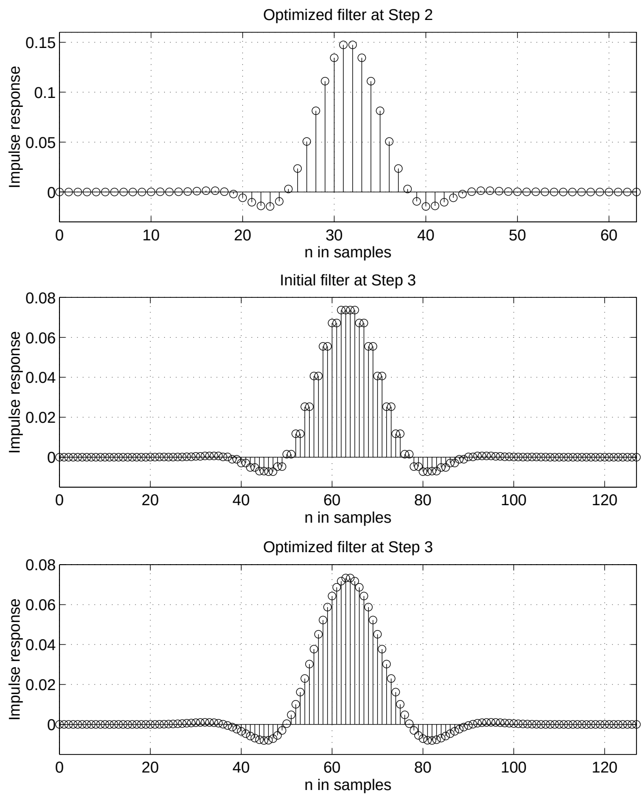

Figure 6: Impulse responses for filters involved when performing Step 3 in the proposed five-step procedure.

Table I: Comparison Between Various Banks of $M = 32$ Filters for $\rho = 1$

- The filter length is $N + 1 = 2KM$
- Boldface numbers show the fixed values.

Design	K	N	δ_1	δ_2	E_∞	E_2
L_2	**8**	**511**	**0**	**0** $-\infty$ dB	$1.2 \cdot 10^{-3}$ -58 dB	$7.4 \cdot 10^{-9}$
L_∞	**8**	**511**	**0**	**0** $-\infty$ dB	$2.3 \cdot 10^{-4}$ -73 dB	$7.5 \cdot 10^{-8}$
L_2	**8**	**511**	**0.0001**	$2.3 \cdot 10^{-6}$ -113 dB	$1.0 \cdot 10^{-5}$ -100 dB	$5.6 \cdot 10^{-13}$
L_∞	**8**	**511**	**0.0001**	$1.1 \cdot 10^{-5}$ -99 dB	$5.1 \cdot 10^{-6}$ -106 dB	$3.8 \cdot 10^{-11}$
L_2	**8**	**511**	**0**	$9.1 \cdot 10^{-5}$ -81 dB	$4.5 \cdot 10^{-4}$ -67 dB	$5.4 \cdot 10^{-10}$
L_2	**8**	**511**	**0.01**	$5.3 \cdot 10^{-7}$ -126 dB	$2.4 \cdot 10^{-6}$ -112 dB	$4.5 \cdot 10^{-14}$
L_2	**6**	**383**	**0.001**	**0.00001** **-100 dB**	$1.7 \cdot 10^{-4}$ -75 dB	$2.8 \cdot 10^{-10}$
L_2	**5**	**319**	**0.01**	**0.0001** **-80 dB**	$8.4 \cdot 10^{-4}$ -62 dB	$2.7 \cdot 10^{-9}$

Figure 7: Least-squared perfect-reconstruction bank of $M = 32$ filters of length $N+1 = 8 \cdot 2M = 512$ for $\rho = 1$.

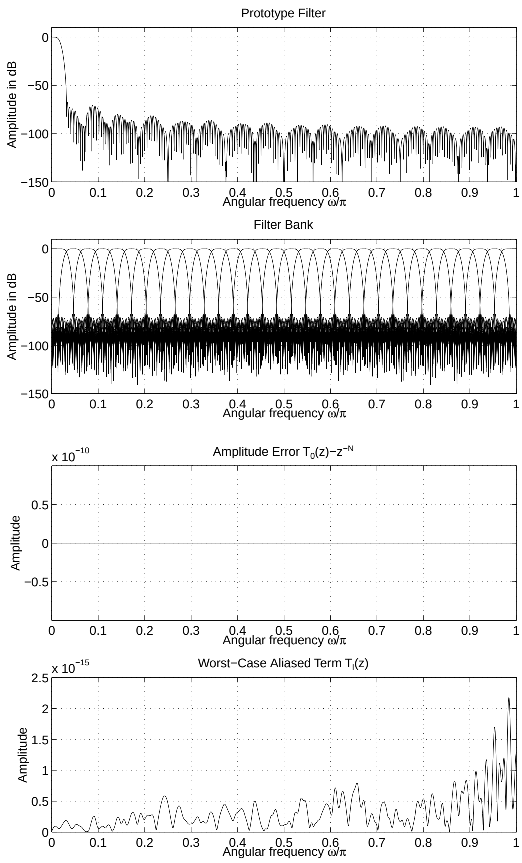

4.6 Design algorithm for problem B

- For Problem B, an efficient synthesis scheme based on the use of the Jing-Fam algorithm [16], [17] has been described in [13].
- Alternatively, the problem can be solved by using the Dutta-Vidyasagar algorithm.
- To do this, we we discretize the region $[\omega_s, \pi]$ into the discrete points $\omega_i \in [\omega_s, \pi]$ for $i = 1, 2, \cdots, I$.
- In many cases, $I = 20N$ is a good selection.
- The resulting discrete minimax problem is to find Φ to minimize

$$\epsilon = \widehat{E}_\infty(\Phi) = \max_{i \in I} f_i(\Phi), \qquad (36a)$$

where

$$f_i(\Phi) = |G_p(\Phi, \omega_i)|, \quad i = 1, 2, \cdots, I. \qquad (36b)$$

- Figure 8 shows in the perfect-reconstruction case the prototype filter designed in the minimax sense as well as the filters in the bank for $M = 32$, $N = 512$, and $\rho = 1$.
- Some characteristics of the resulting filter bank can be found in Table I.
- As can be expected, the minimum stopband attenuation of the prototype filter is significantly higher for the minimax design compared to the least-squared de-

sign (73 dB compared to 58 dB).

- However, for the least-squared design, the stopband energy is considerably lower ($7.4 \cdot 10^{-9}$ compared to $7.5 \cdot 10^{-8}$).

Figure 8: Minimax perfect-reconstruction bank of $M = 32$ filters of length $N+1 = 8 \cdot 2M = 512$ for $\rho = 1$.

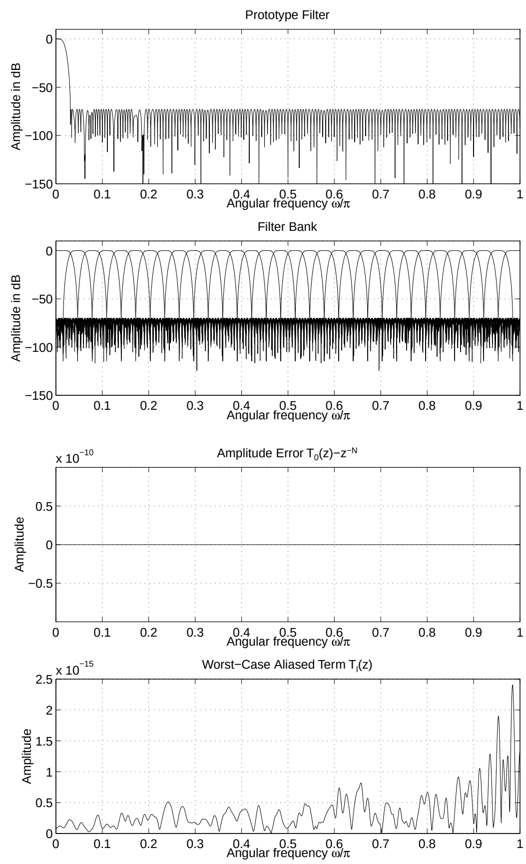

5 Filters with Small Amplitude Distortion $|T_0(e^{j\omega})|$

• Filters with very small aliasing errors can be synthesized by allowing a small amplitude distortion $|T_0(e^{j\omega})|$ for high-order filters.

• This is illustrated in Figs. 9 and 10 for the $M = 32$, $N + 1 = 512$, and $\rho = 1$ case, where $\delta_1 = 0.0001$.

• Figure 9 shows the amplitude responses of the least-squared-error prototype filter and the corresponding filter bank as well as the amplitude response of $T_0(z) - z^{-N}$ and the worst-case aliased term $T_l(z)$.

• The corresponding results for the minimax design are shown in Fig. 10.

• These filters have been optimized without considering the aliasing errors.

• When comparing these responses with those of Figs. 7 and 8, it is seen that the attenuations of both the prototype filter and the filters in the bank have been improved approximately by 40 dB at the expense of very small aliasing errors and a very small amplitude distortion (see also Table I).

• For the least-squared design, $\delta_2 = 2.3 \cdot 10^{-6}$ (113 dB) and for the minimax design, $\delta_2 = 1.1 \cdot 10^{-5}$ (99 dB)

• By allowing a larger value for δ_1, both the filter

bank performance is improved and the aliasing errors become smaller.

• This is illustrated in the least-mean-square case in Figs. 11 and 12 for $\delta_1 = 0$ and $\delta_1 = 0.01$, respectively.

• It is seen from Table I that for the perfect-reconstruction filter as well as for the filters with $\delta_1 = 0$, $\delta_1 = 0.0001$, and $\delta_1 = 0.1$ the mininimum stopband attenuations (the stopband energies) of the prototype filters are 58 dB, 67 dB, 106 dB, and 112 dB, respectively ($7.4 \cdot 10^{-9}$, $5.4 \cdot 10^{-10}$, $5.6 \cdot 10^{-13}$, and $4.5 \cdot 10^{-14}$, respectively).

• The corresponding minimum stopband attenuations of the worst-case aliased transfer functions are ∞ dB, 81 dB, 113 dB, and 126 dB, respectively.

Figure 9: Least-squared bank of $M = 32$ filters of length $N+1 = 8 \cdot 2M = 512$ for $\rho = 1$ and $\delta_1 = 0.0001$.

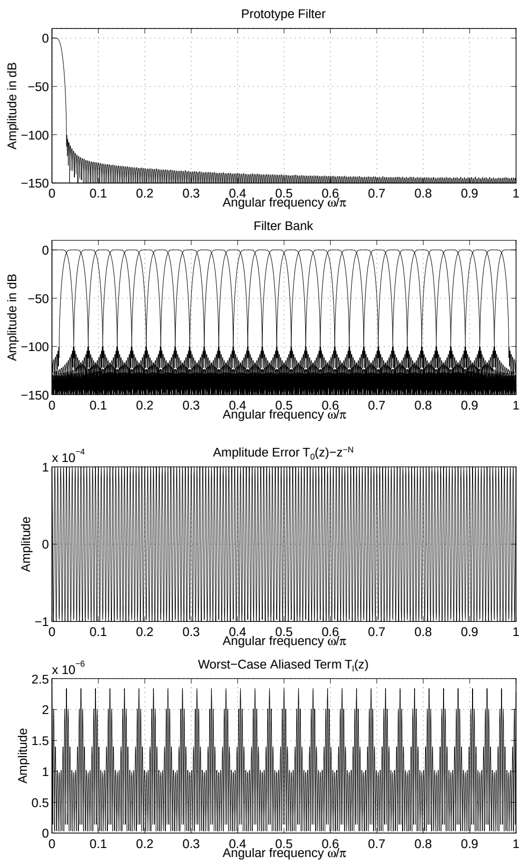

Figure 10: Minimax bank of $M = 32$ filters of length $N+1 = 8 \cdot 2M = 512$ for $\rho = 1$ and $\delta_1 = 0.0001$.

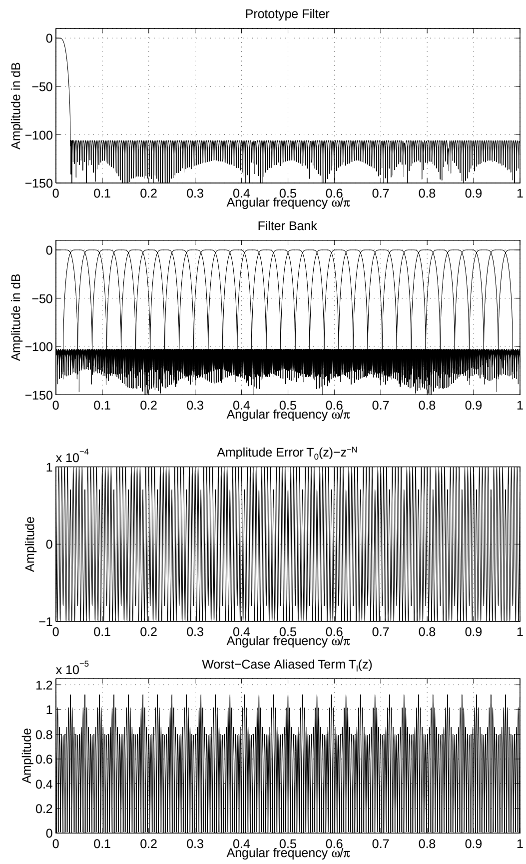

Figure 11: Least-squared bank of $M = 32$ filters of length $N + 1 = 8 \cdot 2M = 512$ for $\rho = 1$ and $\delta_1 = 0$.

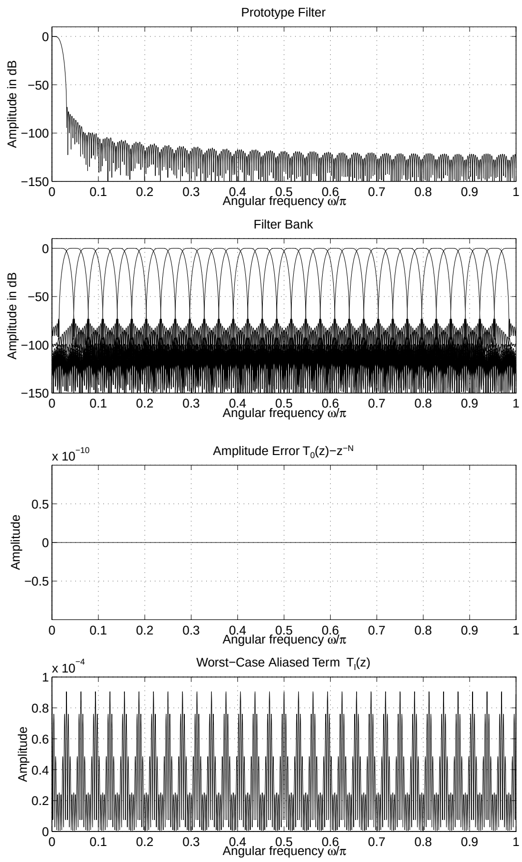

Figure 12: Least-squared bank of $M = 32$ filters of length $N+1 = 8 \cdot 2M = 512$ for $\rho = 1$ and $\delta_1 = 0.01$.

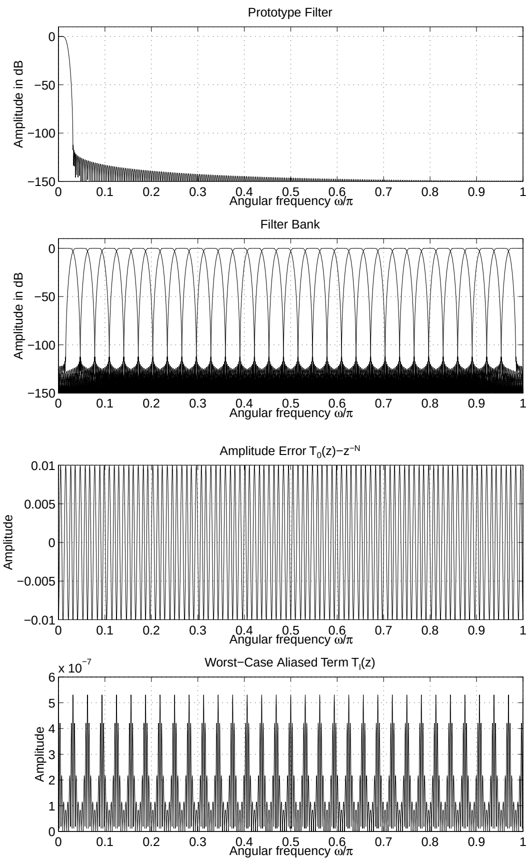

6 General Examples

- This section illustrates, by means of two examples, the flexibility of the general design technique for reducing the lengths of the filters in the bank to achieve practically the same filter bank performance as with the perfect-reconstruction filter banks.
- For both examples, $M = 32$, $\rho = 1$, and the least-mean-square criterion is used for optimizing the prototype filter.
- For the first example, $N + 1 = 384$ $(K = 6)$, $\delta_1 = 0.001$, and $\delta_2 = 10^{-5}$ (a 100-dB attenuation).
- For the second example, $N + 1 = 320$ $(K = 5)$, $\delta_1 = 0.01$, and $\delta_2 = 10^{-4}$ (a 80-dB attenuation).
- Responses for the optimized filters are shown in Figs. 13 and 14, respectively.
- As seen from Table I (or by comparing Figs. 13 and 14 with Fig. 7), these two optimized prototype filters provide a better filter bank performance than the perfect-reconstruction filter band with $N + 1 = 512$ $(K = 8)$.
- The main advantage of the above two filter banks is that the delays caused by them are 383 samples and 319 samples, respectively, compared to 511 samples caused by the perfect-reconstruction filter bank equiva-

lent.

- These figures are directly the orders of the prototype filters.

Figure 13: Least-squared bank of $M = 32$ filters of length $N + 1 = 6 \cdot 2M = 384$ for for $\rho = 1$, $\delta_1 = 0.001$, and $\delta_2 = 0.00001$.

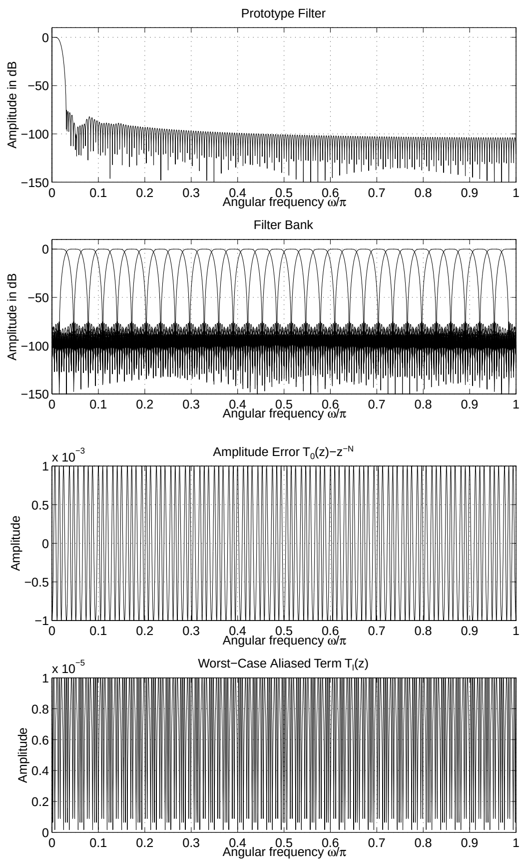

Figure 14: Least-squared bank of $M = 32$ filters of length $N+1 = 5{\cdot}2M = 320$ for for $\rho = 1$, $\delta_1 = 0.01$, and $\delta_2 = 0.0001$.

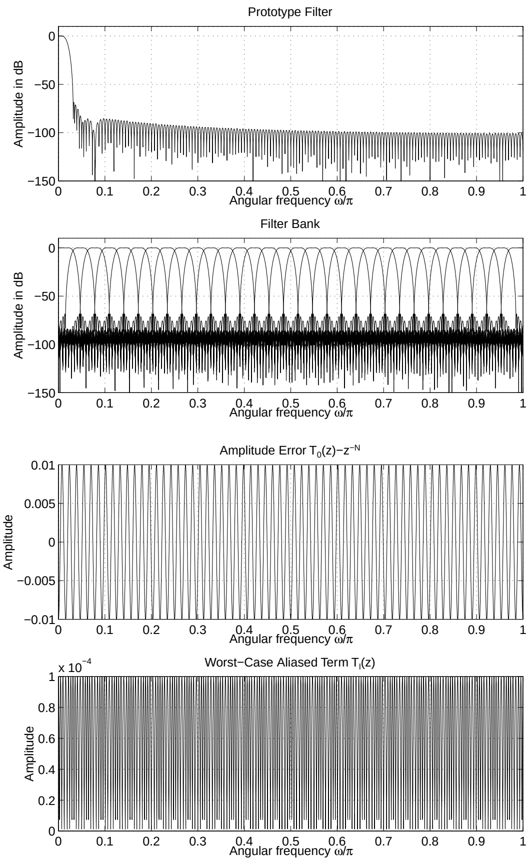

7. Implementation Aspects

• The most effective way of implementing cosine-modulated filter banks has been proposed by Malvar in [1] and [11].

• In this implementation, the protype filter in both the analysis and synthesis part is implemented at the lower sampling rate using special butterflies.

• The cosine modulation is implemented using a DCT IV block.

• In the next version of this pile of lecture notes, more details are included.

References

[1] H. S. Malvar, *Signal Processing with Lapped Transforms.* Norwood: Artech House, 1992.

[2] P. P. Vaidyanathan, *Multirate Systems and Filter Banks.* Englewood Cliffs: Prentice-Hall , 1993.

[3] N. J. Fliege, *Multirate Digital Signal Processing.* Chichester: John Wiley and Sons, 1994.

[4] T. Q. Nguyen, "Near-perfect-reconstruction pseudo-QMF banks," *IEEE Trans. Signal Proc.*, vol. 42, pp. 63–76, Jan. 1994.

[5] F. Mintzer, "On half-band, third-band, and Nth-band FIR filters and their design," *IEEE Trans. Acousts, Speech, Signal Process.*, vol. ASSP-30, pp. 734–738, Oct. 1982.

[6] T. Saramäki and Y. Neuvo, "A class of FIR Nyquist (Nth-Band) filters with zero intersymbol interference," *IEEE Trans. Circuits Syst.*, vol. CAS-34, pp. 1182–1190, Oct. 1987.

[7] S. R. K. Dutta and M. Vidyasagar, "New algorithms for constrained minimax optimization," *Mathematical Programming*, vol. 13, pp. 140–155, 1977.

[8] H. S. Malvar, "Modulated QMF filter banks with perfect reconstruction," *Electron Lett.*, vol. 26, pp. 906–907, June 21, 1990.

[9] T. A. Ramstad and J. P. Tanem, "Cosine-modulated analysis-synthesis filter bank with critical sampling and perfect reconstruction," in *Proc. IEEE Int. Conf. Acoust., Speech, Signal Process.* (Toronto, Canada), pp. 1789–1792, May 1991.

[10] R. D. Koilpillai and P. P. Vaidyanathan, "New results on cosine-modulated FIR filter banks satisfying perfect reconstruction," in *Proc. IEEE Int. Conf. Acoust., Speech, Signal Process.* (Toronto, Canada), pp. 1793–1796, May 1991.

[11] H. S. Malvar, "Extended lapped transforms: Fast algorithms and applications," in *Proc. IEEE Int. Conf. Acoust., Speech, Signal Process.* (Toronto, Canada), pp. 1797–1800, May 1991.

[12] R. D. Koilpillai and P. P. Vaidyanathan, "Cosine-modulated FIR filter banks satisfying perfect reconstruction," *IEEE Trans. Signal Proc.*, vol. 40, pp. 770–783, Apr. 1992.

[13 T. Saramäki, “Designing prototype filters for perfect-reconstruction cosine-modulated filter banks,” in *Proc. 1992 IEEE Int. Symp. Circuits and Syst.* (San Diego, CA), pp. 1605–1608, May 1992.

[14] H. S. Malvar, “Extended lapped transforms: Properties, applications, and fast algorithms,” *IEEE Trans. Signal Proc.*, vol. 40, pp. 2703–2714, Nov. 1992.

[15] R. Fletcher and M. J. D. Powell, “A rapidly convergent descent method for minimization,” Comput. J., vol. 6, pp. 163–168, 1963.

[16] Z. Q. Jing, “Chebyshev design of digital filters by a new minimax algorithm,” Ph. D. dissertation, State University of New York at Buffalo, 1983.

[17] Z. Q. Jing and A. T. Fam, “An algorithm for computing continuous Chebyshev approximations,” *Mathematics of Computation*, vol. 48, pp. 691–710, Apr. 1987